Spatial Coherence in Complex Photonic and Plasmonic Systems

A. Cazé, R. Pierrat, and R. Carminati*

Institut Langevin, ESPCI ParisTech, CNRS, 1 rue Jussieu, 75238 Paris Cedex 05, France

(Received 17 July 2012; published 8 February 2013)

The concept of cross density of states characterizes the intrinsic spatial coherence of complex photonic or plasmonic systems, independently of the illumination conditions. Using this tool and the associated intrinsic coherence length, we demonstrate unambiguously the spatial squeezing of eigenmodes on disordered fractal metallic films, thus clarifying a basic issue in plasmonics.

DOI: 10.1103/PhysRevLett.110.063903 PACS numbers: 42.25.Dd, 32.50.+d, 73.20.Mf, 78.67.−n

The optical properties of nanostructured materials have attracted a lot of attention due to their potential for light concentration and transport at subwavelength scales [1,2]. New possibilities have emerged for the design of efficient sources and absorbers of visible and near-infrared radiation, or for optical storage and information processing with ultrahigh spatial density. Metallic nanostructures benefit from the excitation of surface plasmons that permit concentration at ultrasmall length scales and ultrafast time scales [3]. Disordered media also offer the possibility to build up spatially localized modes (e.g., by the process of Anderson localization) [4]. Light concentration and transport at subwavelength scales encompass a broad range of processes, including coherent control at the nanoscale [5], enhancement of light-matter interaction in weak and strong coupling regimes [6–10], superradiance [11], enhancement of nonradiative energy transfer [12], or light focusing beyond the diffraction limit [13–15]. The spatial extent of eigenmodes is of central importance, since it characterizes the ability of the system to support concentrated or delocalized excitations. It drives, e.g., the coherence length of surface plasmons [10,16–19], the range of nonradiative energy transfer [20,21], or the lower limit for spatial focusing by time reversal or phase conjugation [22–24]. The trade-off between localized and delocalized excitations is also a central issue for the understanding and the control of the optical properties of disordered fractal metallic films [25]. In this Letter, we introduce the cross density of states (CDOS) as a quantity that characterizes the overall spatial extent of eigenmodes, and use it to address the spatial localization of light on disordered fractal metallic films. We demonstrate unambiguously the spatial squeezing of eigenmodes close to the percolation threshold, thus providing a theoretical basis to clarify a controversial issue in plasmonics [6,26–28]. This also illustrates the relevance of the CDOS to characterize the intrinsic spatial coherence in photonics and plasmonics systems.

In order to characterize the intrinsic spatial coherence of a complex photonic or plasmonic system at a given frequency ω, we introduce a two-point quantity $\rho(\mathbf{r}, \mathbf{r}', \omega)$ that we will refer to as CDOS, defined as

$$\rho(\mathbf{r}, \mathbf{r}', \omega) = \frac{2\omega}{\pi c^2} \mathrm{Im}[\mathrm{Tr}\mathbf{G}(\mathbf{r}, \mathbf{r}', \omega)]. \quad (1)$$

In this expression, c is the speed of light in vacuum, $\mathbf{G}(\mathbf{r}, \mathbf{r}', \omega)$ is the electric dyadic Green function that connects the electric field at point $\mathbf{r}$ to an electric-dipole source $\mathbf{p}$ at point $\mathbf{r}'$ through the relation $\mathbf{E}(\mathbf{r}) = \mu_0\omega^2\mathbf{G}(\mathbf{r}, \mathbf{r}', \omega)\mathbf{p}$, and Tr denotes the trace of a tensor.

The choice of this quantity as a measure of the intrinsic spatial coherence results from the observation that the imaginary part of the Green function at two different points appears in a number of situations where the spatial coherence of random fields (produced by random sources and/or a disordered medium) needs to be characterized [4,29–31]. The imaginary part of the Green function also describes the process of focusing by time reversal in a closed cavity [22,23]. The precise definition of the CDOS in Eq. (1) has been chosen so that it reduces to the local density of states (LDOS) when $\mathbf{r}$ and $\mathbf{r}'$ coincide [2,32].

The physical picture behind the CDOS is a counting of optical eigenmodes that connect two different points at a given frequency. In a network picture, the LDOS measures the number of channels crossing at a given point, whereas the CDOS measures the number of channels connecting two points. In order to give a more rigorous basis to this picture, let us first consider the canonical situation of a nonabsorbing system (e.g., a nanostructured material) placed in a closed cavity. In this case, using an orthonormal discrete basis of eigenmodes with eigenfrequencies ω_n and eigenvectors $\mathbf{e}_n(\mathbf{r})$, the CDOS defined by Eq. (1) can be rewritten as [33]:

$$\rho(\mathbf{r}, \mathbf{r}', \omega) = \sum_n \mathrm{Tr}[\mathbf{e}_n^*(\mathbf{r}', \omega)\mathbf{e}_n(\mathbf{r}, \omega)]\delta(\omega - \omega_n). \quad (2)$$

This expression explicitly shows that the CDOS sums up all eigenmodes connecting $\mathbf{r}$ to $\mathbf{r}'$ at frequency ω, weighted by their strength at both points $\mathbf{r}$ and $\mathbf{r}'$. In the case of an open and/or absorbing system, as that considered in the present study, the rigorous introduction of a basis of eigenmodes is more involved. Approaches have been developed in the quasistatic limit [34], or based on statistical properties of the spectral decomposition of non-Hermitian matrices [35]. Assuming weak leakage, one can also use

a phenomenological approach in which quasimodes are introduced by broadening the eigenmodes using a linewidth γ_n. This results in an expansion similar to (2) with a Lorentzian line shape replacing the delta function [33]. This generalizes the physical picture to lossy systems. Nevertheless, it is important to note that all calculations presented in this Letter are performed using Eq. (1), in which the correct counting of modes is implicit, without referring to a basis of eigenmodes.

We shall now show that the concept of CDOS allows us to clarify an important issue in nanophotonics concerning light scattering and localization in disordered fractal metallic films. These peculiar structures exhibit optical properties that strongly differ from those of bulk metals or ensembles of isolated nanoparticles [25]. In particular, the multiscale geometry of percolation clusters induces long-range correlations that make simple models (e.g., white-noise potentials or homogenization procedures) invalid. The interplay between surface-plasmon resonances and multiple scattering by the fractal percolation clusters leads to spatial concentration of light in subwavelength areas (hot spots) [36,37]. The theoretical description of this phenomenon has been the subject of controversy. Using a scaling theory in the quasi-static limit, a mechanism based on Anderson localization has been put forward [38]. Anderson localization on percolating systems for electronic (quantum) transport leads to a clear transition between the localized and delocalized regimes [39]. For light scattering on percolating metallic systems, a theoretical analysis has proved the existence of localized modes characterized by algebraic rather than by exponential spatial confinement, and that can be coupled to radiation [35]. Numerical simulations on planar random composites have even shown that localized and delocalized plasmonic eigenmodes could coexist [26]. This has been confirmed by measurements and computations of intensity fluctuations in the near field [27,28], that have also indicated that localized modes should dominate around the percolation threshold (but not exactly at percolation). More recently, measurements of near-field LDOS statistics have confirmed the existence of spatially localized modes in the regime dominated by fractal clusters (close to the percolation threshold) [6]. For nanophotonics, a major issue is the description of the overall spatial extent of *the full set* of eigenmodes whatever the underlying mechanism (regarding this issue, the coexistence of localized and delocalized modes is not a central point). Spatial coherence and the concept of CDOS appear as natural tools to address this issue, as we shall see. We will introduce the intrinsic coherence length as a measure of this overall spatial extent. This gives a new point of view for the description of light localization on disordered metallic films.

The CDOS can be calculated numerically using exact three-dimensional simulations. We summarize the procedure that is fully described in Ref. [40]. Semicontinuous gold films are generated using a kinetic Monte Carlo algorithm, reproducing the geometrical features of real films. Typical realizations of films are shown in the top row in Fig. 1 (with gold in black color), each film being 5 nm thick and lying in free space. To calculate the electric dyadic Green function $\mathbf{G}(\mathbf{r}, \mathbf{r}', \omega)$, we need to calculate the electric field at a position $\mathbf{r}$ generated by a point electric-dipole source $\mathbf{p}$ located at position $\mathbf{r}'$. To proceed, we solve numerically the Lippmann-Schwinger equation:

$$\mathbf{E}(\mathbf{r}) = \mathbf{E}_0(\mathbf{r}) + \frac{\omega^2}{c^2} \int [\epsilon(\mathbf{r}', \omega) - 1]\mathbf{G}_0(\mathbf{r}, \mathbf{r}', \omega)\mathbf{E}(\mathbf{r}')d^3r' \tag{3}$$

where $\mathbf{G}_0$ is the vacuum dyadic Green function, $\mathbf{E}_0(\mathbf{r})$ the incident field and $\epsilon(\mathbf{r}, \omega)$ the dielectric function. The full dyadic Green function is deduced from $\mathbf{E}(\mathbf{r}) = \mu_0\omega^2\mathbf{G}(\mathbf{r}, \mathbf{r}', \omega)\mathbf{p}$. The computation of the LDOS and CDOS follows from Eq. (1).

We show in Fig. 1 the LDOS maps (middle row) and CDOS maps (bottom row) computed in a plane at a distance $z = 40$ nm above two different films (shown in the top row) corresponding to two different regimes.

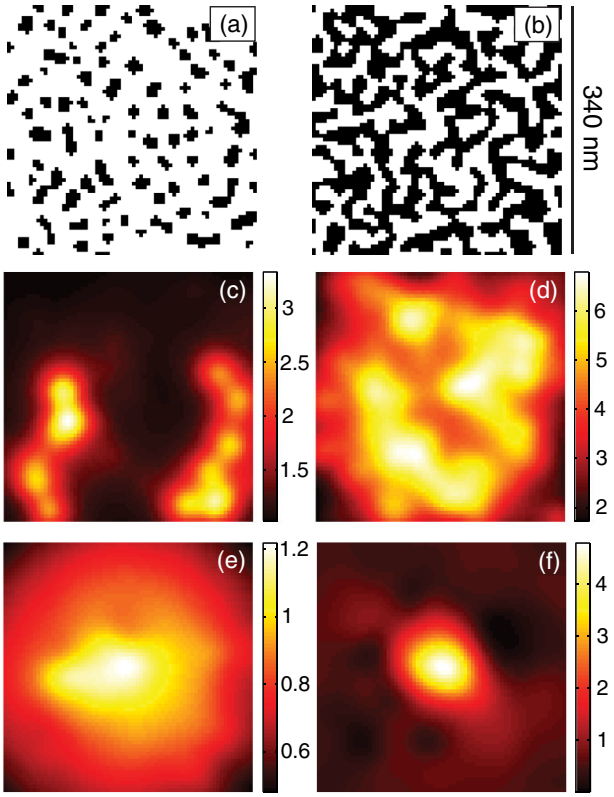

FIG. 1 (color online). (a),(b): Geometry of the disordered films generated numerically (with gold in black color). (a): $f = 20\%$, (b): $f = 50\%$. (c),(d): Maps of the normalized LDOS $\rho(\mathbf{r}, \omega)/\rho_0(\omega)$ calculated in a plane at a distance $z = 40$ nm above the film surface, $\rho_0(\omega)$ being the LDOS in vacuum. (e),(f): Maps of the normalized CDOS $\rho(\mathbf{r}, \mathbf{r}', \omega)/\rho_0(\omega)$ with $\mathbf{r}'$ fixed at the center of the sample. $\lambda = 780$ nm.

For $f = 20\%$ (left column), the film is composed of isolated nanoparticles whereas for $f = 50\%$ (right column) the film is slightly below the percolation threshold (from numerical simulations, this threshold is estimated at $f = 53\%$), a regime in which fractal clusters dominate (multiscale resonant regime) [6,25,40]. Before studying spatial coherence and the extent of eigenmodes based on the CDOS, let us summarize here the main features of the LDOS maps [21,40]. For low surface fraction (left column), LDOS peaks are observed on top of isolated nanoparticles that are resonant at the observation wavelength. A correspondence between LDOS peaks and the position of one or several nanoparticles is easily made. For a different observation wavelength (not shown for brevity), particles can switch on or off resonance and the position of the LDOS peaks changes, but remain attached to individual particles. The sample behaves as a collection of individual nanoparticles with well-identified surface plasmon resonances. In the multiscale resonant regime (right column), the LDOS structure is more complex. There is no obvious correspondence between the film topography (composed of fractal clusters in which the concept of individual nanoparticles becomes meaningless) and the localized field enhancements responsible for LDOS fluctuations. This is a known feature of fractal metallic films [26,36,37,41].

The maps of the CDOS $\rho(\mathbf{r}, \mathbf{r}', \omega)$ (bottom row in Fig. 1) are displayed versus $\mathbf{r}$ for a fixed position $\mathbf{r}'$ (chosen at the center of the sample). Their meaning can be understood as follows: They display the ability of a point $\mathbf{r}$ at a given distance from the center point $\mathbf{r}'$ to be connected to this center point by the underlying structure of the optical eigenmodes. For example, a large CDOS (larger than the vacuum CDOS) would allow two quantum emitters at $\mathbf{r}$ and $\mathbf{r}'$ to couple efficiently. It would also ensure coherent (correlated) fluctuations of the light fields at $\mathbf{r}$ and $\mathbf{r}'$ under thermal excitation [29]. The CDOS also allows one to discriminate between two hot spots at $\mathbf{r}$ and $\mathbf{r}'$ that belong to the same eigenmode (or that are connected by at least one eigenmode), or that are completely independent. Last but not least, since the CDOS implicitly sums up the spatial extent of the full set of eigenmodes, it appears as a natural tool to describe the overall spatial localization in the multiscale resonant regime. It is striking to see that the extent of the CDOS in the multiscale resonant regime [Fig. 1(f)] is reduced to a smaller range compared to the case of a film composed of isolated nanoparticles [Fig. 1(e)]. The reduction of the extent of the CDOS clearly demonstrates an overall spatial squeezing of the eigenmodes close to the percolation threshold (remember that the CDOS is implicitly a weighted sum over the full set of eigenmodes). Let us stress that the approach based on the CDOS gives a nonambiguous description of this overall spatial squeezing, whatever the underlying mechanism. It is based on a concept implicitly related to field-field spatial correlations as in classical spatial coherence theory, that seems to carry sufficient information to describe one of the most striking features in the optics of disordered fractal metallic films.

In order to quantify the overall reduction of the spatial extent of eigenmodes in the multiscale resonant regime, we introduce an intrinsic coherence length ℓ_{coh}, defined from the width of the CDOS. More precisely, fixing $\mathbf{r}'$ at the center of the sample, we use polar coordinates in the plane $z = 40$ nm parallel to the sample mean surface to write $\rho(\mathbf{r}, \mathbf{r}', \omega) = \rho(R, \theta, \omega)$ with $R = |\mathbf{r} - \mathbf{r}'|$ and define an angularly averaged CDOS $\bar{\rho}(R, \omega) = (2\pi)^{-1} \times \int_0^{2\pi} \rho(R, \theta, \omega) d\theta$. The intrinsic coherence length ℓ_{coh} is defined as the half width at half maximum of $\bar{\rho}(R, \omega)$ considered as a function of R. It is important to note that ℓ_{coh} is not necessarily the size of the hot spots observed on the surface, since a given eigenmode can be composed of several hot spots. Two different hot spots separated by a distance smaller than ℓ_{coh} can be intrinsically connected (meaning that they are connected by at least one eigenmode). The ability to clarify this distinction between eigenmodes and hot spots is an essential feature of the CDOS. The averaged value of $\langle \ell_{\mathrm{coh}} \rangle$ and its variance $\mathrm{Var}(\ell_{\mathrm{coh}})$ (error bars) are shown in Fig. 2 versus the film surface fraction for two wavelengths, $\lambda = 650$ nm and $\lambda = 780$ nm. Both quantities are calculated using a statistical ensemble of realizations of disordered films generated numerically (the error bars indicate the real variance of ℓ_{coh}, and not computations errors due to lack of numerical convergence, the latter being ensured by a sufficiently large set of realizations). For both wavelengths, the average value $\langle \ell_{\mathrm{coh}} \rangle$ is significantly smaller near the percolation threshold than for lower filling fractions. This unambiguously demonstrates the overall spatial squeezing of eigenmodes in the regime dominated by fractal clusters, with a stronger squeezing at $\lambda = 780$ nm

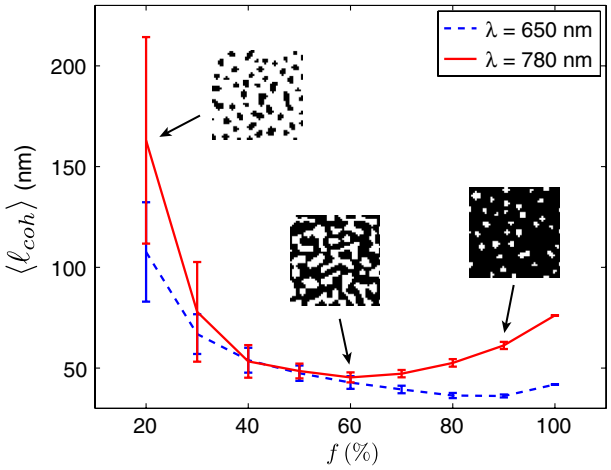

FIG. 2 (color online). Averaged value and variance (error bars) of the intrinsic coherence length ℓ_{coh} calculated at a distance $z = 40$ nm above a disordered film, versus the gold surface fraction f. Inset: Typical film geometries (black color corresponds to gold).

where more pronounced resonances occur [25]. The curve for $\lambda = 780$ nm even shows a minimum near the percolation threshold. Our approach provides a theoretical description of the experiment in Ref. [6], although in this study, the inverse participation ratio was used to connect qualitatively the spatial extent of eigenmodes to the variance of the LDOS fluctuations. Therefore only a qualitative comparison with the curve in Fig. 2 is possible (the inverse participation ratio and the intrinsic coherence length cannot be compared directly). Moreover, the precise shape of the calculated curves might also be influenced by finite-size effects inherent to the numerical simulation. The behavior of $\mathrm{Var}(\ell_{\mathrm{coh}})$ is also instructive. Strong fluctuations are observed in the regime of isolated nanoparticles. In this regime, optical modes attached to a single particle and delocalized modes are observed, which is different from the known behavior in quantum electronic transport [39]. The strong fluctuations reflect the fluctuations in the interparticle distance. Conversely, in the multiscale resonant regime, the reduction of the fluctuations reinforces the assumption of a mechanism based on collective interactions that involve the sample as a whole.

In summary, we have shown that the CDOS characterizes the intrinsic spatial coherence of a photonic or plasmonic system, independently on the illumination conditions. Using this concept, we have demonstrated unambiguously the spatial squeezing of plasmonic eigenmodes on disordered fractal metallic films close to the percolation threshold. This clarifies a basic issue in plasmonics concerning the description of the optical properties of these films. This illustrates the relevance of the CDOS in the study of spatial coherence in photonics and plasmonics systems, and more generally in wave physics.

We acknowledge Y. De Wilde, M. Kociak, V. Krachmalnicoff, and R. Sapienza for stimulating discussions.

*remi.carminati@espci.fr

[1] U. Kreibig and M. Vollmer, *Optical Properties of Metal Clusters* (Springer, Berlin, 1995).
[2] L. Novotny and B. Hecht, *Principles of Nano-Optics* (Cambridge University Press, Cambridge, England, 2006).
[3] M. I. Stockman, Opt. Express **19**, 22029 (2011).
[4] P. Sheng, *Introduction to Wave Scattering, Localization, and Mesoscopic Phenomena* (Academic Press, San Diego, 1995).
[5] M. Durach, A. Rusina, and M. I. Stockman, Nano Lett. **7**, 3145 (2007).
[6] V. Krachmalnicoff, E. Castanié, Y. De Wilde, and R. Carminati, Phys. Rev. Lett. **105**, 183901 (2010).
[7] L. Sapienza, H. Thyrrestrup, S. Stobbe, P. D. Garcia, S. Smolka, and P. Lodahl, Science **327**, 1352 (2010).
[8] R. Sapienza, P. Bondareff, R. Pierrat, B. Habert, R. Carminati, and N. van Hulst, Phys. Rev. Lett. **106**, 163902 (2011).
[9] D. E. Chang, A. S. Sorensen, E. A. Demler, and M. D. Lukin, Nat. Phys. **3**, 807 (2007).
[10] S. A. Guebrou, C. Symonds, E. Homeyer, J. Plenet, Yu. Gartstein, V. Agranovich, and J. Bellessa, Phys. Rev. Lett. **108**, 066401 (2012).
[11] P. A. Huidobro, A. Y. Nikitin, C. González-Ballestero, L. Martín-Moreno, and F. J. García-Vidal, Phys. Rev. B **85**, 155438 (2012).
[12] J. Seelig, K. Leslie, A. Renn, S. Kühn, V. Jacobsen, M. van de Corput, C. Wyman, and V. Sandoghdar, Nano Lett. **7**, 685 (2007).
[13] X. Li and M. I. Stockman, Phys. Rev. B **77**, 195109 (2008).
[14] A. Sentenac and P. C. Chaumet, Phys. Rev. Lett. **101**, 013901 (2008).
[15] I. M. Vellekoop, A. Lagendijk, and A. P. Mosk, Nat. Photonics **4**, 320 (2010).
[16] J. Verbeecka, D. van Dycka, H. Lichteb, P. Potapova, and P. Schattschneider, Ultramicroscopy **102**, 239 (2005).
[17] Y. De Wilde, F. Formanek, R. Carminati, B. Gralak, P.-A. Lemoine, K. Joulain, J.-P. Mulet, Y. Chen, and J.-J. Greffet, Nature (London) **444**, 740 (2006).
[18] A. Trügler, J.-C. Tinguely, J. R. Krenn, A. Hohenau, and U. Hohenester, Phys. Rev. B **83**, 081412(R) (2011).
[19] S. Mazucco, N. Geuquet, J. Ye, O. Stéphan, W. Van Roy, P. Van Dorpe, L. Henrard, and M. Kociak, Nano Lett. **12**, 1288 (2012).
[20] R. Vincent and R. Carminati, Phys. Rev. B **83**, 165426 (2011).
[21] E. Castanié, V. Krachmalnicoff, A. Cazé, R. Pierrat, Y. De Wilde, and R. Carminati, Opt. Lett. **37**, 3006 (2012).
[22] J. de Rosny and M. Fink, Phys. Rev. Lett. **89**, 124301 (2002).
[23] R. Carminati, R. Pierrat, J. de Rosny, and M. Fink, Opt. Lett. **32**, 3107 (2007).
[24] G. Lerosey, J. de Rosny, A. Tourin, and M. Fink, Science **315**, 1120 (2007).
[25] V. M. Shalaev, *Nonlinear Optics of Random Media* (Springer, Berlin, 2000).
[26] M. I. Stockman, S. V. Faleev, and D. J. Bergman, Phys. Rev. Lett. **87**, 167401 (2001).
[27] K. Seal, D. Genov, A. Sarychev, H. Noh, V. Shalaev, Z. Ying, X. Zhang, and H. Cao, Phys. Rev. Lett. **97**, 206103 (2006).
[28] D. A. Genov, A. K. Sarychev, and V. M. Shalaev, Phys. Rev. E **67**, 056611 (2003).
[29] K. Joulain, J. P. Mulet, F. Marquier, R. Carminati, and J.-J. Greffet, Surf. Sci. Rep. **57**, 59 (2005).
[30] R. L. Weaver and O. I. Lobkis, Phys. Rev. Lett. **87**, 134301 (2001); E. Larose, L. Margerin, A. Derode, B. van Tiggelen, M. Campillo, N. Shapiro, A. Paul, L. Stehly, and M. Tanter, Geophysics **71**, S11 (2006).
[31] T. Setälä, K. Blomstedt, M. Kaivola, and A. T. Friberg, Phys. Rev. E **67**, 026613 (2003).
[32] The LDOS $\rho(\mathbf{r}, \omega) = 2\omega/(\pi c^2)\mathrm{Im}[\mathrm{Tr}\mathbf{G}(\mathbf{r}, \mathbf{r}, \omega)]$ enters the expression of the spontaneous decay rate of an electric dipole [2]. For magnetic dipole transitions, or for the computation of equilibrium energy density, an additional magnetic term has to be added, see K. Joulain,

R. Carminati, J. P. Mulet, and J.-J. Greffet, Phys. Rev. B **68**, 245405 (2003).
[33] See Supplemental Material at http://link.aps.org/supplemental/10.1103/PhysRevLett.110.063903 for the derivation of the eigenmode expansion of the CDOS.
[34] G. Boudarham and M. Kociak, Phys. Rev. B **85**, 245447 (2012).
[35] V. A. Markel, J. Phys. Condens. Matter **18**, 11149 (2006).
[36] S. Grésillon, L. Aigouy, A. Boccara, J. Rivoal, X. Quelin, C. Desmarest, P. Gadenne, V. Shubin, A. Sarychev, and V. Shalaev, Phys. Rev. Lett. **82**, 4520 (1999).
[37] J. Laverdant, S. Buil, B. Bérini, and X. Quélin, Phys. Rev. B **77**, 165406 (2008).
[38] A. K. Sarychev, V. A. Shubin, and V. M. Shalaev, Phys. Rev. B **60**, 16389 (1999).
[39] C. M. Soukoulis, Q. Li, and G. S. Grest, Phys. Rev. B **45**, 7724 (1992); I. Chang, Z. Lev, A. B. Harris, J. Adler, and A. Aharony, Phys. Rev. Lett. **74**, 2094 (1995).
[40] A. Cazé, R. Pierrat, and R. Carminati, Photon. Nanostr. Fundam. Appl. **10**, 339 (2012).
[41] C. Awada, G. Barbillon, F. Charra, L. Douillard, and J.-J. Greffet, Phys. Rev. B **85**, 045438 (2012).